Investigation of the Anistropy of Surface-Emitted Longwave Radiation Using Satellite and Airborne Instrument Data

M. M. Khaiyer, S. Mayor, L. Nguyen, W. L. Smith, Jr., and D. R. Doelling
Analytical Services and Materials, Inc.
Hampton, Virginia

P. Minnis
Atmospheric Sciences Division
National Aeronautics and Space Administration
Langley Research Center
Hampton, Virginia

L. Egli
Swiss Federal Institute of Technology
Zurich, Switzerland

Introduction

The derivation of land surface skin temperature from satellite and airborne instruments is crucial for many applications, including the calculation of outgoing longwave radiation (OLR). Heavy reliance is placed on measurements from these instruments, but typically these are available from only a single viewing direction. Since it is difficult to obtain measurements viewing the same area from different directions, the factors that can bias single-view values must be understood. Failing to account for anisotropic emission of longwave radiation is a significant, but rarely recognized factor that can lead to errors in parameters derived from the measurements over clear land areas. Rugged terrain or surface vegetation can cause shadowing that leads to a variation in measured temperature depending on the location of the detector.

A number of recent studies have examined this effect, and found significant brightness temperature differences (BTDs) depending on various angular and surface characteristics. Lipton and Ward (1997) examined the effects of rugged terrain by simulating satellite data using temperatures derived from models with high-resolution terrain data, and found that such terrain led to high temperature biases. Minnis and Khaiyer (1999) used coincident, multi-angle Geostationary Operational Environmental Satellite (GOES) infrared (IR) window (10.8 μm) brightness temperature data from April-May 1998 to evaluate longwave radiance anisotropy. The results revealed significant daytime BTDs that depend on terrain and vegetation type, as well as the viewing and illumination angles. Calculation of OLR from the different brightness temperatures revealed a significant error, ranging between 15 W/m^2 and -11 W/m^2. The study further determined that BTDs were closely related to shortwave bidirectional reflectance distribution functions (BRDFs) and topography. Thus, these factors may be useful for

deriving a parameterization of the anisotropy. However, this determination was constrained to data from a single season, spatial scale, and a few sets of angles. Therefore, GOES data covering the annual cycle, as well as airborne data from the MAS (Moderate-Resolution Imaging Spectroradiometer [MODIS] Airborne Simulator), are added here to evaluate the dependence of IR anisotropy on BRDFs and terrain information for additional seasons and spatial scales.

Methodology

This study uses GOES IR radiances taken over clear areas for selected days during 1995-1998, and MAS IR data taken with the National Aeronautics and Space Administration (NASA) ER-2 during the fall 1995 ARESE (ARM [Atmospheric Radiation Measurement] Enhanced Shortwave Experiment). All of the GOES images were manually corrected for navigational errors by matching coastlines and/or flat-land features, and were calibrated by matching GOES-West and GOES-East data at the midpoint between the two satellites at solar noon and/or late at night. Clear regions were chosen from days during all four seasons. The GOES data were separated into 2° by 2° regions and subdivided into 10-ft. boxes that were characterized by International Geosphere Biosphere Programme (IGBP) scene type. There were a limited number of clear-sky regions for each season. Spring was represented by twelve regions, autumn and summer by three each, and winter by two. GOES-7, -8, -9, and -10 (if available for the chosen days) IR radiances were then averaged within each 10-ft. box, and were corrected for atmospheric attenuation with a radiative transfer model using absorption optical depths from the correlated k-distribution method of Kratz (1995). The radiances were then converted to an effective surface brightness temperature (BT) with the Planck function. Thus, a single average brightness temperature per IGBP scene type represents each 2° x 2° region for a given satellite.

Two procedures were used to analyze the MAS data. In both cases, the MAS radiances are corrected for atmospheric attenuation in the same manner as the GOES data. The first approach compares the GOES and MAS temperatures, while the second examines the variation of the MAS data across scan lines. To compare the MAS and GOES data, the MAS channel-45 (11-μm) pixel radiances (~50-m resolution) within the approximate boundaries of a given GOES pixel (~4-km resolution) were averaged together to obtain a single MAS BT. The MAS and GOES BTs were correlated for selected flights over the Gulf of Mexico to develop a procedure for normalizing the MAS and GOES temperatures. The correlation and resulting regression line shown in Figure 1 are based on collocated GOES and MAS data taken at similar viewing zenith and relative azimuth angles. The line, which reveals a MAS cold bias ranging from 0.3 K to 1.0 K between 300 K and 250 K, respectively, was used to adjust the MAS data taken over land. BTDs between MAS and GOES were computed for each GOES pixel.

Because the MAS is a cross-track scanner, each pixel in a scan line is viewed with a different viewing zenith angle (VZA). Therefore, to determine the dependence of temperature on viewing and illumination conditions, radiances corresponding to a constant scan position over a long flight track were averaged together to obtain a single BT composed of similar scene types for all scan positions. The difference of the MAS nadir and off-nadir BTs was calculated for each scan position.

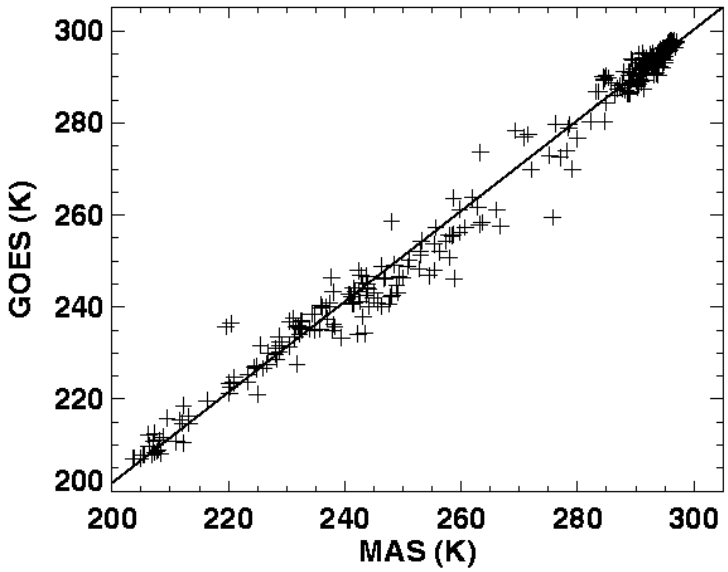

Figure 1. Correlation of collocated brightness temperatures from GOES-8 and the ER-2 MAS taken over the Gulf of Mexico during September and October 1995.

Results

Time series of GOES-8, -9, and -10 brightness temperatures during April 1998 reveal curves that peak around local noon with hourly differences that depend on the solar and satellite azimuth angles (not shown). This effect is further illustrated by a seasonal comparison of BTDs from GOES- East (75°W) and GOES-West (135°W) for flat grassland during autumn, spring, and summer days (Figure 2). These curves show striking peaks in the morning, when the eastern satellite views few shadows, and minima in the afternoon when GOES-West views fewer shadows. The curves show a slightly bigger range in BTD for spring 1998 that may be due to increased vegetation or to stronger solar heating. A comparison of data from rugged-terrain grassland for winter and summer (not shown) shows a similar trend, but exhibits a slightly larger diurnal range in BTD for those respective months.

The BRDFs used by Minnis and Khaiyer (1999) provide a relative measure of the angular dependence of solar illumination on the land surface. Figure 2 reveals a high correlation (squared linear correlation coefficient r^2 ranging between 0.93 and 0.97) between the BTDs for GOES-East and -West and the corresponding differences $\Delta\chi$ in the BRDF anisotropic reflectance factors χ. The slopes of the linear regression fits increase with increasing terrain and vegetation morphology as seen in Figure 3 where the slopes of all BTD versus $\Delta\chi$ line fits are plotted against the standard deviation of terrain height. Linear regression fits were computed between the BTD versus $\Delta\chi$ slopes and elevation standard deviation separately for data from each season. The correlations are fairly significant for all seasons (squared linear correlation coefficient, $r^2 = 0.65 - 0.96$).

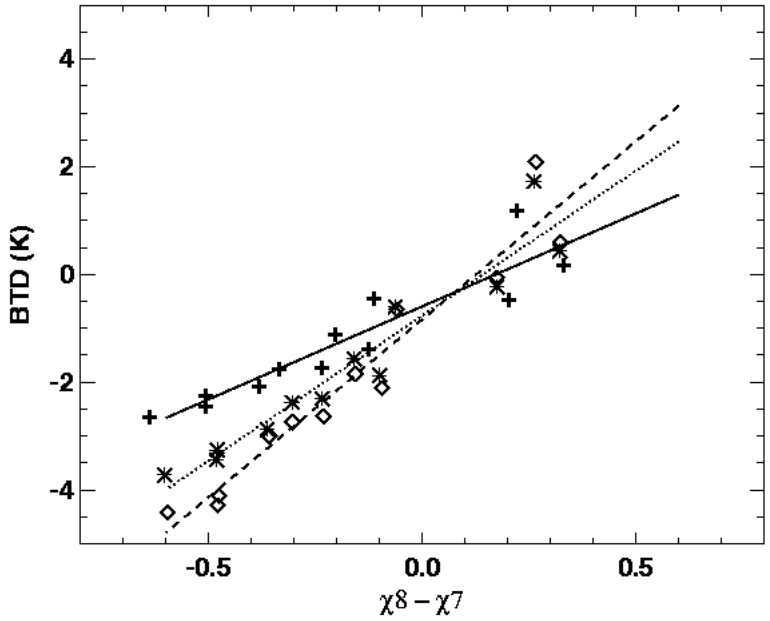

Figure 2. Correlations of differences in brightness temperature and BRDF (GOES-East - GOES-West) for various terrain types, October 14-15, 1995. Solid line denotes flat grassland at 33.5°N, 103.5°W; dotted denotes mountainous grassland at 36°N, 106°W; and dashed shows mountainous forest at 36°N, 106°W.

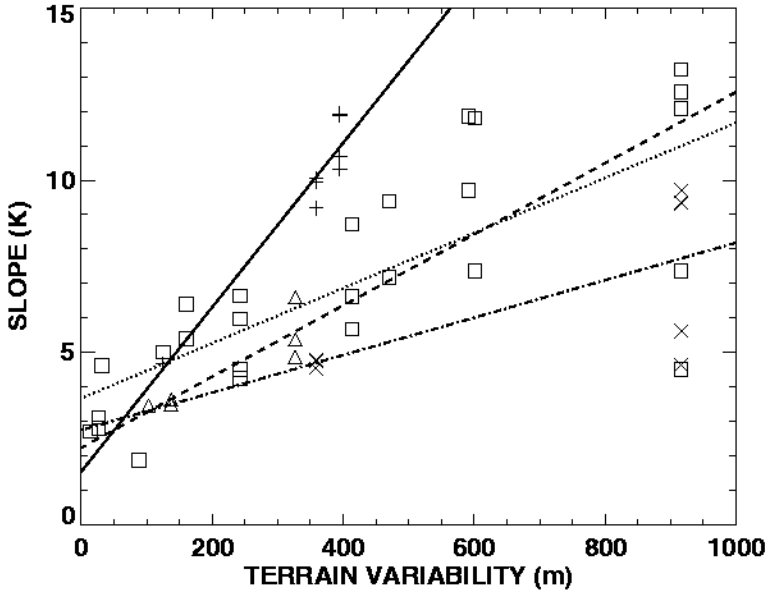

Figure 3. Correlations of line-fit slopes with standard deviation of terrain. Solid line (plus symbols) denotes spring 1998, dashed (triangles) denotes summer 1995, dotted (squares) denotes autumn 1995, and dot-dashed (crosses) denotes winter 1999.

The MAS-GOES BTDs vary systematically with VZA, as illustrated with data obtained in a four-leg pattern flown over mountainous terrain in New Mexico (Figure 4). For example, the scan-position-average BTDs for the north leg of this box are close to zero (Figure 5) where the VZA of MAS most closely matches that of GOES-8. The BTD increases as the MAS VZA turns to the south toward GOES, into more shadowed surfaces. The other legs yield a similar pattern.

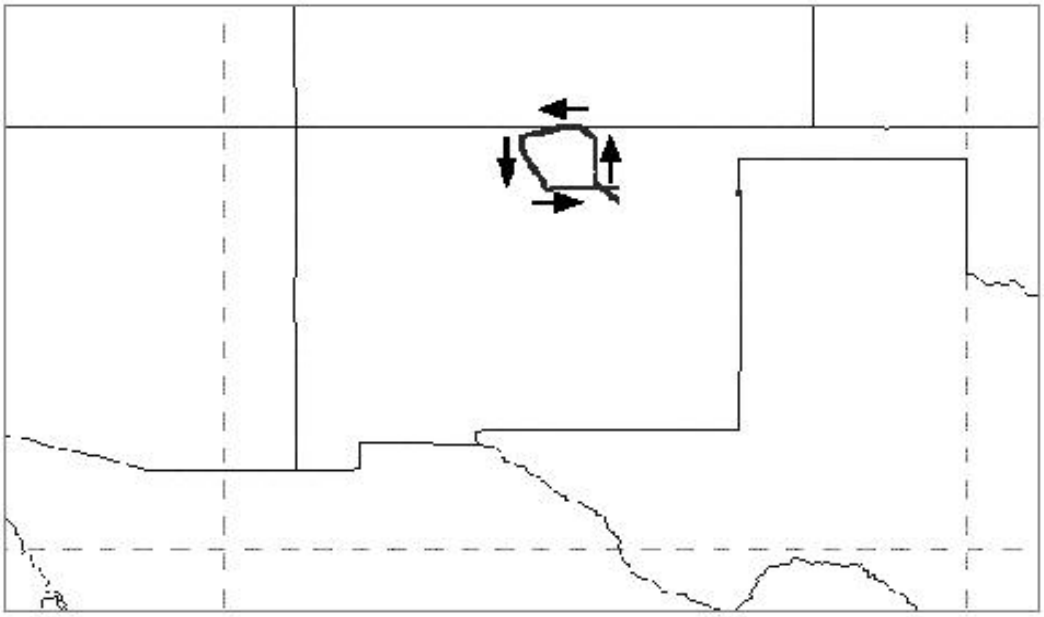

Figure 4. Flight tracks of the ER-2 over New Mexico for October 14, 1995. The box pattern is initiated in the southeast corner (36°N 105°W) at 1745 Universal Time Coordinates (UTC), and is completed at 1820 UTC.

Comparison of MAS nadir and oblique-VZA temperatures show a similar dependence of BTD on VZA. Regression of those BTDs with the appropriate values of $\Delta\chi$ (not shown) reveals a high correlation ($r^2 = 0.82$).

Discussion

The diurnal variations of BTD (Figure 6), the findings of earlier studies, and the view-direction dependence of the MAS data together confirm that longwave emission is anisotropic over land during daylight hours. This anisotropy should be taken into account when IR or broadband longwave radiances are converted to flux or skin temperature. The high correlation of BTD and $\Delta\chi$ (Figure 3) indicates that BRDFs can be used as a factor in predicting anisotropy. These two parameters were correlated for each IGBP type that comprises more than 10% of a 2° x 2° region. The correlation coefficients ranged from 0.81 to 0.96 for autumn, 0.79 to 0.97 for summer, 0.93 to 0.99 for winter, and 0.58 to 0.99 for spring. These results demonstrate that $\Delta\chi$ provides a relative measure of shadowing, which is probably the

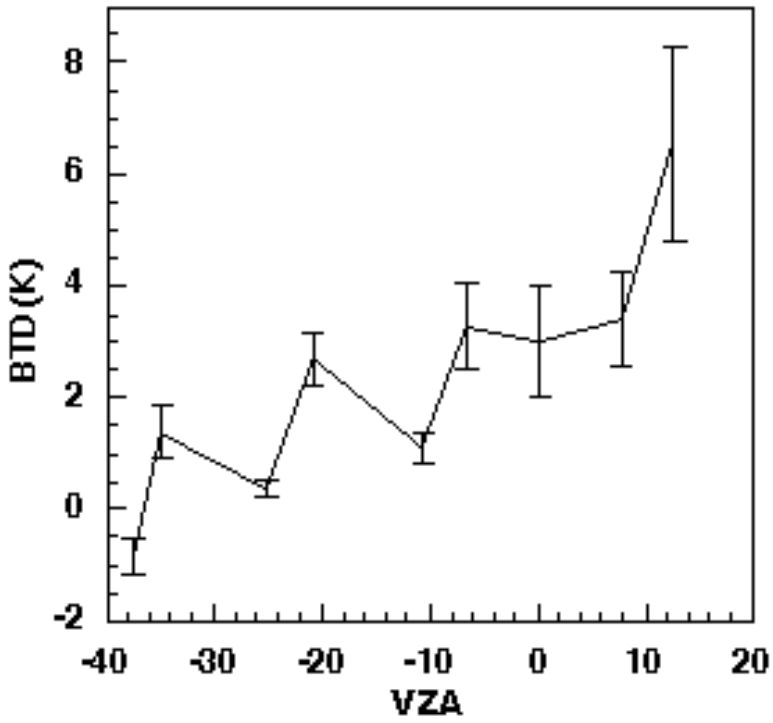

Figure 5. Dependence of GOES-8 - MAS *BTD* with MAS *VZA* for October 14, 1995, north leg of box pattern in Figure 4 (approx. 1756 UTC). MAS scan is from north to south.

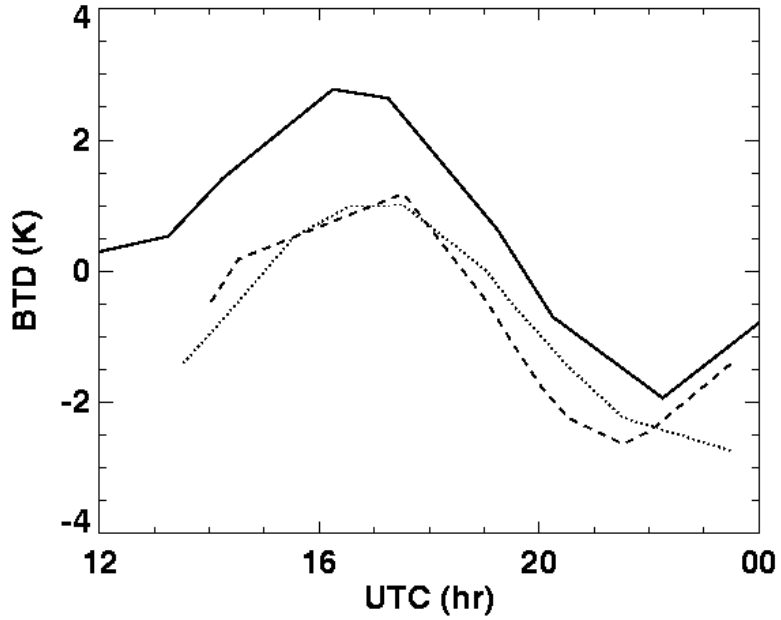

Figure 6. Seasonal variation of GOES-East - GOES-West brightness temperature differences. Autumn 1995 is dashed, summer 1995 is dotted, and spring 1998 is solid.

greatest factor causing the BTD variation. Except at rather large VZAs, the greatest solar reflectance (largest χ) occurs in the anti-solar or direct backscatter position and the minimum solar reflectance (smallest χ) is found in some part of the forward hemisphere where shadows are dominant.

Ideally, the relative degree of shadowing for a given location could be described with a BRDF model developed specifically for that location. Such a model would account for the morphology of the land surface as well as the relative distribution of the vegetation and its morphology. However, current BRDF models are quite generic, representing, at some unknown degree of accuracy, the bidirectional reflectance of a few vegetation types over relatively flat surfaces. Presumably, the magnitudes of anisotropy and shadowing would scale with the frequency and depth of undulations in the land surface. Larger, steeper mountains or narrow canyon walls cast longer, deeper shadows than trees, bushes, or grass. Thus, the surface morphology and vegetation type can serve as a measure of the deviation of localized BRDFs from the generic models. This idea is confirmed by the strong correlations between the standard deviation of elevation (a measure of surface morphology) and the line-fit slopes in Figure 4.

Certainly, other variables such as humidity and wind will also affect the skin temperature and influence the anisotropy of IR radiance. Many more samples are needed to determine the impacts of these other variables.

Conclusions and Future Work

Analysis of GOES data throughout the annual cycle, as well as additional MAS data, confirms that brightness temperatures vary significantly with regard to topography and angular characteristics with some dependency on vegetation cover. Significant correlations between BTDs and corresponding $\Delta\chi$ for both GOES and MAS data sets indicate that BRDF should be useful in the parameterization of longwave anisotropy. An additional dependence on terrain variability was demonstrated with high correlations between slopes of BTD-$\Delta\chi$ line fits and terrain variability (standard deviation of terrain) for the GOES data sets of most seasons. However, the data sets used in this study were limited in amount of clear-sky data available. To further evaluate BRDF and terrain variability for use in predicting longwave anisotropy, the relationship between IR radiance and viewing and illumination angles must be studied for additional flat and rugged regions for all seasons.

It is clear that several independent variables can serve as predictors for the IR anisotropy. However, the formulation of a model that uses these variables to predict the IR radiance must be developed. With additional data and consideration of the theoretical aspects of the source of the anisotropy, it should be possible to construct a robust parameterization of the angular dependence of infrared radiance emitted from most land surfaces.

Acknowledgments

Support for this research was provided by the U.S. Department of Energy Environmental Sciences Division Interagency Agreement #DE-AI02-97ER62341.

References

Kratz, D. P., 1995: The correlated k-distribution techniques as applied to the AVHRR channels. *J. Quant. Spectrosc. Rad. Transfer*, **53**, 501-507.

Lipton, A., and J. Ward, 1997: Satellite-view biases in retrieved surface temperatures in mountain areas. *Remote Sens. Environ*., **60**, 92-100.

Minnis, P., and M. M. Khaiyer, 1999: Anisotropy of land surface skin temperature derived from satellite data. *J. Appl. Meteor*. Submitted.